European Review for Medical and Pharmacological Sciences 2020; 24: 8635-8641

MiR-126 facilitates apoptosis of retinal ganglion cells in glaucoma rats *via* VEGF-Notch signaling pathway

L.-J. WANG[1], X.-Z. WANG[2], Z.-M. LI[3], D. KOU[3], D. ZHANG[4], Z.-Z. XU[5]

[1]Department of Ophthalmology, Yantaishan Hospital, Yantai, China
[2]Department of Pediatrics, Zaozhuang Hospital of Traditional Chinese Medicine, Zaozhuang, China
[3]Department of Health Management, PLA Rocket Force Characteristic Medical Center, Beijing, China
[4]Endoscopy Center, PLA Rocket Force Characteristic Medical Center, Beijing, China
[5]Department of Surgery, Zaozhuang Hospital of Traditional Chinese Medicine, Zaozhuang, China

Abstract. – OBJECTIVE: The aim of this study was to explore the effect of micro ribonucleic acid (miR)-126 on the apoptosis of retinal ganglion cells in glaucoma rats *via* the vascular endothelial growth factor (VEGF)-Notch signaling pathway.

MATERIALS AND METHODS: A total of 36 Sprague-Dawley (SD) rats were randomly divided into three groups, including normal group (n=12), model group (n=12) and miR-126 antagomir group (n=12). Rats in normal group did not receive any treatment. In model group and miR-126 antagomir group, the rats were used to establish glaucoma models and intervened with normal saline and miR-126 antagomir, respectively. Intraocular pressure was detected at the completion of modeling and the last intervention, at 7 days after which samples were taken. Western blotting was adopted to detect the relative protein expressions of Notch1 and Notch2. The content of VEGF was examined via enzyme-linked immunosorbent assay (ELISA). Quantitative polymerase chain reaction (qPCR) was carried out to detect the messenger RNA (mRNA) expressions of VEGF, Notch1 and Notch2. Terminal deoxynucleotidyl transferase dUTP nick end labeling (TUNEL) assay was performed to detect cell apoptosis.

RESULTS: After modeling, intraocular pressure in model group and miR-126 antagomir group was significantly higher than that in normal group ($p<0.05$). At the end of the intervention, intraocular pressure in miR-126 antagomir group was notably lower than that in model group ($p<0.05$). VEGF content in model group and miR-126 antagomir group was notably higher than that in normal group ($p<0.05$). However, it was markedly lower in miR-126 antagomir group than model group ($p<0.05$). Model group exhibited remarkably higher protein expressions of Notch1 and Notch2 than normal group ($p<0.05$). However, the protein expressions of Notch1 and Notch2 in miR-126 antagomir group were evidently reduced ($p<0.05$). Besides, the mRNA expressions of VEGF, Notch1 and Notch2 in model group were significantly higher than those in normal group ($p<0.05$). However, they were significantly lower in miR-126 antagomir group than those in model group ($p<0.05$). Furthermore, the apoptosis rate in model group was distinctly higher than that in normal group ($p<0.05$). However, it was notably lower in miR-126 antagomir group than model group ($p<0.05$).

CONCLUSIONS: MiR-126 facilitates the apoptosis of retinal ganglion cells in glaucoma rats by promoting the VEGF-Notch signaling pathway.

Key Words:
Glaucoma, Retinal ganglion cells, MiR-126, VEGF-Notch signaling pathway, Apoptosis.

Introduction

Glaucoma, a relatively common ophthalmic disease in clinic, is characterized by intraocular hypertension. It affects retinal ganglion tissues to influence vision. Meanwhile, glaucoma is also a vital disease leading to blindness in affected patients. Currently, glaucoma has become the world's number one blinding disease. Insomnia caused by glaucoma seriously affects the labor ability, quality of life and health of patients[1-3]. In recent years, effective treatment and improvement of glaucoma have become a global hotspot and difficulty.

Apoptosis of retinal ganglion cells is a pivotal part of the pathological mechanisms of glaucoma. It is also a crucial pathological factor and cause of insomnia. The vascular endothelial growth factor (VEGF)-Notch signaling pathway is abnormally

Corresponding Author: Zhenzheng Xu, BM; e-mail: 15562237881@qq.com

expressed in neovascular glaucoma, exerting an indispensable effect. Meanwhile, it is one of the mechanisms regulating the apoptosis of numerous retinal ganglion cells[4,5].

Micro ribonucleic acid (MiR)-126 is an important member of the miRNA family in the body. Currently, it is recognized that miR-126 exerts vital regulatory effects in such pathological processes as cell proliferation, apoptosis and necrosis[6,7]. Hence, it is believed that miR-126 participates and plays an important regulatory role in the apoptosis of retinal ganglion cells in the pathological process of glaucoma. In this study, therefore, we explored the effect of miR-126 on the apoptosis of retinal ganglion cells in glaucoma rats through the VEGF-Notch signaling pathway.

Materials and Methods

Laboratory Animals

A total of 36 specific pathogen free (SPF)-grade Sprague-Dawley (SD) rats aged 1 month old were purchased from Shanghai SLAC Laboratory Animal Co., Ltd. [License No.: SCXK (Shanghai, China) 2014-0003]. All rats were fed in The Laboratory Animal Center with normal feed and sterile filtered water daily under the conditions of a 12:12 h light/dark cycle, as well as normal room temperature and humidity. Experiments were conducted after 7 days of adaptive feeding. This investigation was approved by the Animal Ethics Committee of Yantaishan Hospital Animal Center.

Laboratory Reagents

MiR-126 antagomir was purchased from MCE (Monmouth Junction, NJ, USA). Primary antibodies against Notch1 and Notch2 and the corresponding secondary antibodies were bought from Abcam (Cambridge, MA, USA). Nissol stain kits and enzyme-linked immunosorbent assay (ELISA) kits were provided by Beyotime (Shanghai, China). Moreover, kits for terminal deoxynucleotidyl transferase dUTP nick end labeling (TUNEL) assay and quantitative polymerase chain reaction (qPCR) were purchased from Vazyme (Nanjing, China).

Animal Grouping and Treatment

The above-mentioned SD rats were randomly assigned into three groups using a random number table, including normal group (n=12), model group (n=12) and miR-92a antagomir group (n=12). Rats in normal group did not receive any treatment. Rats in model group were utilized to establish the model of glaucoma-induced acute intraocular hypertension and intraperitoneally injected with normal saline every day after operation. Meanwhile, rats in miR-126 antagomir were applied to construct the model of glaucoma-induced acute intraocular hypertension and intraperitoneally injected with 3 μM of miR-126 antagomir daily after operation. The samples were taken after the intervention for 7 consecutive days in each group.

Modeling of Glaucoma-Induced Acute Intraocular Hypertension

The rats were first intraperitoneally injected with 3% pentobarbital sodium solution at a dose of 5 mL/kg. After successful anesthesia, they were placed in the prone position, and the anterior chamber was punctured through the corneal limbus using a lateral penetrating knife under an operation microscope. Next, 0.1 mL of aqueous humor in the anterior chamber was extracted using a syringe along the lateral penetrating knife. About 0.1 mL of viscoelastic agents were injected to prepare the model of glaucoma-induced acute intraocular hypertension.

Measurement of Intraocular Pressure

The rats were intraperitoneally injected with 3% pentobarbital sodium solution at the completion of modeling and the last intervention, with an injection dose of 5 mL/kg. After successful anesthesia, the intraocular pressure of each rat was measured independently by two testers using a portable tonometer, and the average value was recorded.

Sampling

Anesthesia was performed by intraperitoneal injection of 3% pentobarbital sodium solution (5 mL/kg). After successful anesthesia, 6 rats in each group underwent direct sampling. Briefly, retinal tissues were directly taken out, washed with normal saline and put into an Eppendorf (EP) tube for storage at -80°C. The remaining 6 rats were fixed by perfusion for sampling. Specifically, 400 mL of 4% paraformaldehyde was perfused from the left atrial appendage, and retinal tissues were taken out and fixed with 4% paraformaldehyde solution.

Western Blotting

Retinal tissues preserved at ultra-low temperature were added with lysate and subjected to ice bath for 1 h, followed by centrifugation for 10 min at 14000 g. Protein concentration was deter-

mined by the bicinchoninic acid (BCA) method (Pierce, Rockford, IL, USA). Subsequently, protein samples were separated by sodium dodecyl sulphate-polyacrylamide gel electrophoresis (SDS-PAGE) gel electrophoresis, and the position of Marker proteins was observed. When Marker proteins were in a straight line at the bottom of a glass plate, the electrophoresis was terminated. Next, the proteins were transferred onto polyvinylidene difluoride (PVDF) membranes (Millipore, Billerica, MA, USA). After reaction with blocking solution for 1.5 h, the membranes were incubated with primary antibodies against RhoA (1:1000) and ROCK1 (1:1000) overnight. On the next day, the membranes were incubated with corresponding secondary antibodies (1:1000) for 2 h at room temperature. Immunoreactive bands were fully developed in the dark using a chemiluminescent reagent for 1 min.

Detection of Inflammatory Factors in Retinal Tissues Via ELISA

Freshly taken tissues were first minced. According to the instructions of the ELISA kits, samples were loaded, and standards, biotinylated antibody working fluid and enzyme conjugate working fluid were added. Next, the plates were fully washed. Absorbance at 450 nm was finally detected by a micro-plate reader.

Quantitative Polymerase Chain Reaction (qPCR)

Total RNAs were extracted from fresh tissues using TRIzol extraction reagent. Subsequently, extracted RNA was reversely transcribed into complementary deoxyribose nucleic acids (cDNAs) using a reverse transcription kit. The qPCR system (20 μL) was designed, and the reaction conditions were as follows: reaction at 53°C for 5 min, pre-denaturation at 95°C for 10 min, denaturation at 95°C for 10 s and annealing at 62°C for 30 s, for a total of 35 cycles. Next, ΔCt value was calculated to determine the expression of target genes. Primer sequences used in this study were shown in Table I.

Terminal Deoxynucleotidyl Transferase dUTP Nick End Labeling (TUNEL)

Paraffin-embedded tissues were sliced into 5 μm-thick sections, flattened in warm water at 42°C, fished up, baked and prepared into paraffin sections. The sections were sequentially soaked in xylene solution and alcohol with a gradient concentration for conventional deparaffinization and hydration. Apoptosis was finally examined according to the instructions of TUNEL assay kits.

Statistical Analysis

Statistical Product and Service Solutions (SPSS) 20.0 software (IBM, Armonk, NY, USA) was adopted for statistical analysis. Count data were expressed as mean ± standard deviation. Data conforming to normal distribution and homogeneity of variance were detected by *t*-test, those conforming to normal distribution and heterogeneity of variance were examined *via* corrected *t*-test, and those not conforming to normal distribution and homogeneity of variance were detected using non-parametric test. Rank-sum test was carried out for ranked data, and chi-square test for count data. p-value < 0.05 was considered statistically significant.

Results

Intraocular Pressure in Each Group

After modeling, intraocular pressure in model group and miR-126 antagomir group was significantly higher than that in normal group, showing statistically significant differences ($p<0.05$). At the end of the intervention, intraocular pressure in miR-126 antagomir group was notably lower than that in model group, displaying a statistically significant difference ($p<0.05$) (Figure 1).

Table I. Primer sequences.

Name	Primer sequence
VEGF	Forward primer: 5'CATGCGGATCAAACCTCACC3' Reverse primer: 5'TCACCGCCTTGGCTTGTCAC3'
Notch1	Forward primer: 5'GCTCCGAGGAGATCAACGAG3' Reverse primer: 5'TTGACATCACCCTCACACCG3'
Notch2	Forward primer: 5'AGAGTCTGCCTCAGCCTTAG3' Reverse primer: 5'AGAGTCTGCCTCAGCCTTAG3'
GAPDH	Forward primer: 5'ACGGCAAGTTCAACGGCACAG3' Reverse primer: 5'GAAGACGCCAGTAGACTCCACGAC3'

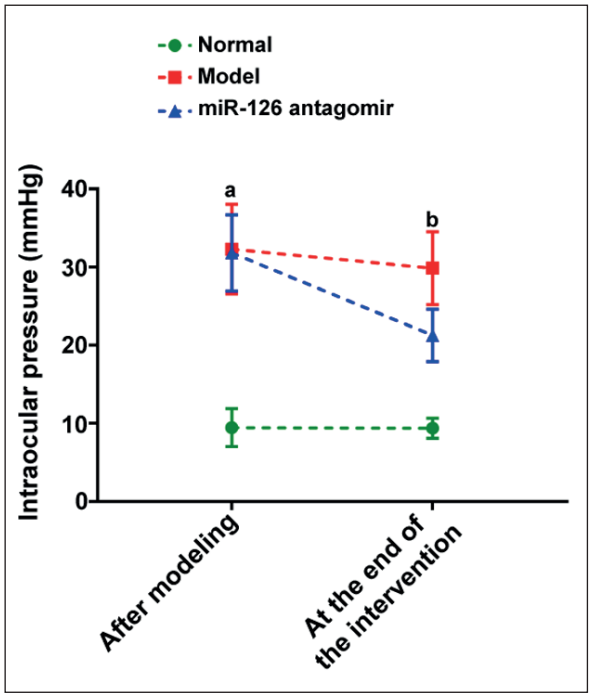

Figure 1. Intraocular pressure in each group. Note: p^a<0.05 *vs.* normal group, and p^b<0.05 *vs.* model group.

VEGF Content Detected Via ELISA

VEGF content in model group and miR-126 antagomir group was notably higher than that in normal group, with statistically significant differences (p<0.05). However, it was markedly lower in miR-126 antagomir group than that in model group (p<0.05) (Figure 2).

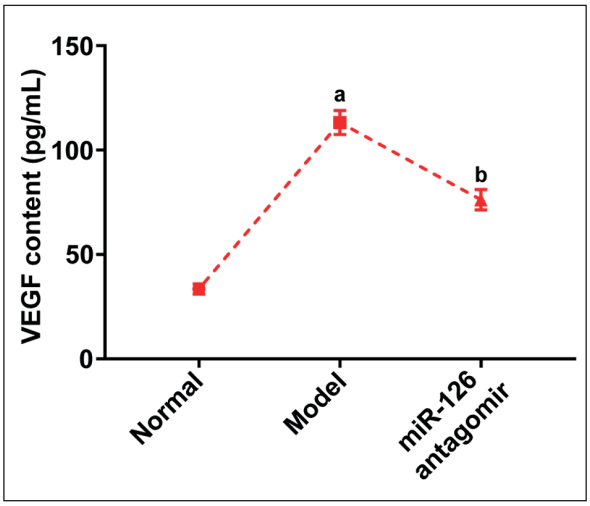

Figure 2. VEGF content in each group. Note: p^a<0.05 *vs.* normal group, and p^b<0.05 *vs.* model group.

Protein Expression Examined by Western Blotting

As shown in Figure 3A, the protein expressions of Notch1 and Notch2 were relatively low in normal group and high in model group. It could be observed that model group exhibited remarkably higher protein expressions of Notch1 and Notch2 than normal group, and the differences were statistically significant (p<0.05). Besides, the protein expressions of Notch1 and Notch2 in miR-126 antagomir group were evidently reduced, with statistically significant differences (p<0.05) (Figure 3B).

Messenger RNA (mRNA) Expression Measured Via qPCR

The mRNA expressions of VEGF, Notch1 and Notch2 in model group were prominently higher than those in normal group (p<0.05). However, they were remarkably lower in miR-126 antagomir group than those in model group, exhibiting statistically significant differences (p<0.05) (Figure 4).

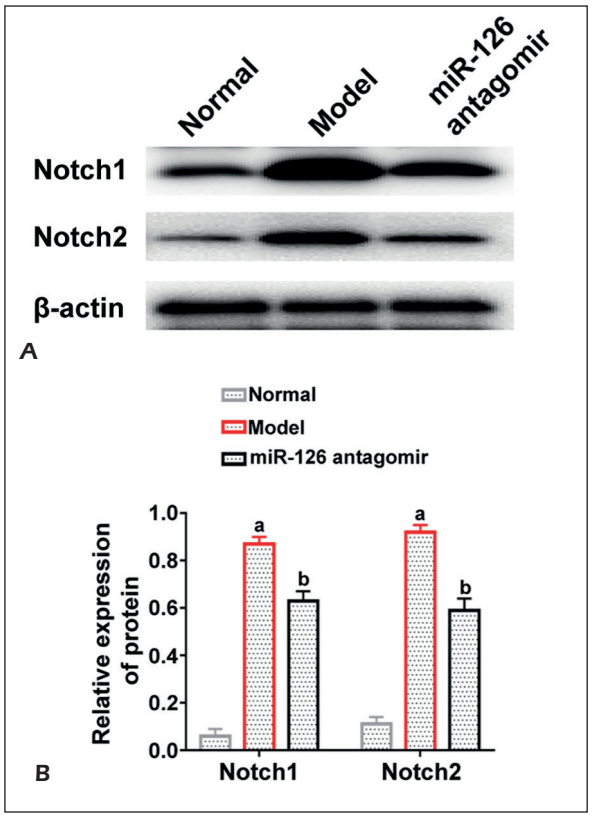

Figure 3. Relative protein expression in each group. Note: (A) Protein expression band diagrams, and (B) Statistical results of the relative expression of related proteins. Note: p^a<0.05 *vs.* normal group, and p^b<0.05 *vs.* model group.

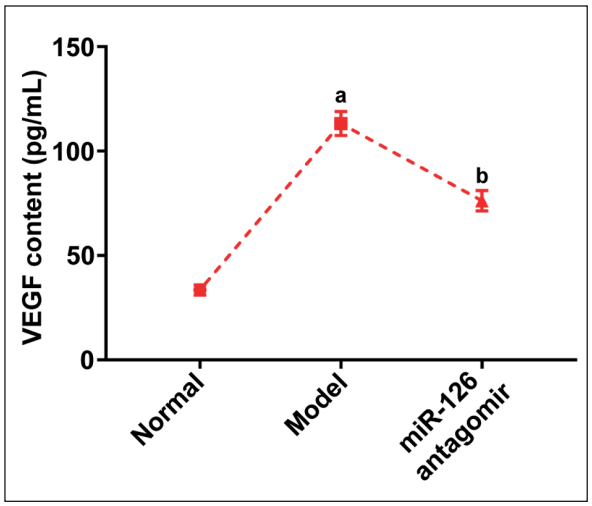

Figure 4. Relative mRNA expression in each group. Note: $p^a<0.05$ *vs.* normal group, and $p^b<0.05$ *vs.* model group.

Apoptosis Detected Via TUNEL Assay

Apoptotic cells were green, and there were fewer TUNEL-positive apoptotic cells in normal group and more in model group (Figure 5A). As shown in Figure 5B, the apoptosis rate in normal group was markedly higher than that in normal group, and the difference was statistically significant ($p<0.05$). Besides, the apoptosis rate in miR-126 antagomir group was evidently lower than that in model group, showing a statistically significant difference ($p<0.05$).

Discussion

The global number of disabilities caused by glaucoma has doubled in the elderly within 10 years, with a dramatically increasing incidence rate. Glaucoma is a very common clinical ophthalmic disease, whose main features include optic nerve injury and visual field defect. It is pathologically characterized by acute intraocular hypertension. Acute intraocular hypertension is the most important pathological factor of glaucoma as well as a crucial pathological cause of visual impairment[8-10]. In the case of acute intraocular hypertension, retinal tissues may undergo ischemia, hypoxia and edema. Meanwhile, the release of numerous cytokines and inflammatory factors can give rise to apoptosis, necrosis, autophagy and other pathological conditions of a large number of retinal ganglion cells. Hence, the apoptosis of retinal ganglion cells caused by acute intraocular hypertension is an important pathological mechanism and process of glaucoma. This exerts vital effects on the structure and function of these

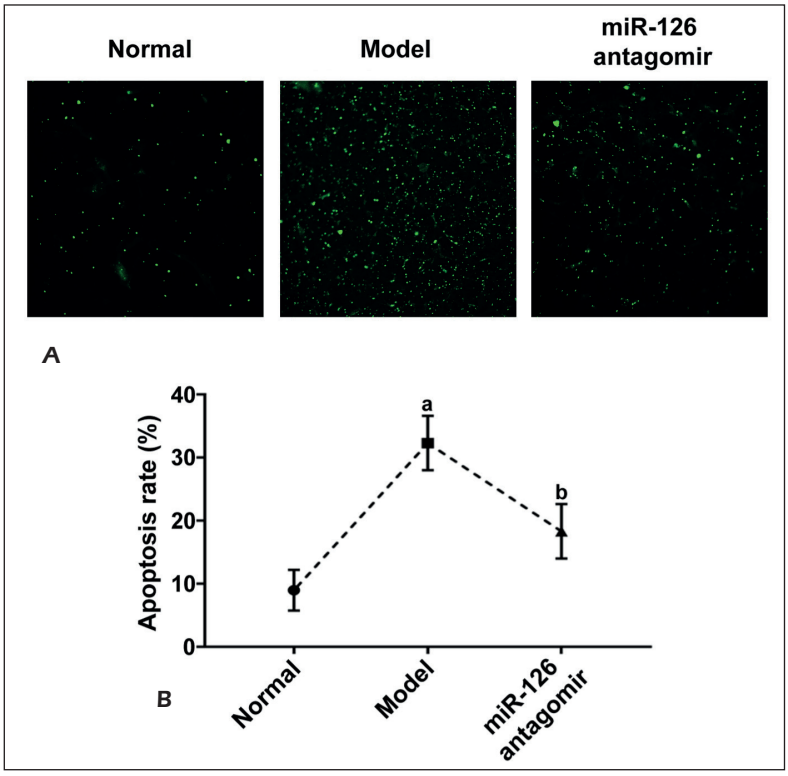

Figure 5. Apoptosis detected via TUNEL assay. Note: (**A**) Apoptosis examined via TUNEL assay (magnification: 400×) (**B**) Apoptosis rate in each group. Note: $p^a<0.05$ *vs.* normal group, and $p^b<0.05$ *vs.* model group.

cells, which is also a pivotal factor influencing the recovery of glaucoma and reducing vision damage. Intervention and regulation of the apoptosis of retinal ganglion cells induced by acute intraocular hypertension can effectively reduce visual impairment, so as to protect retinal ganglion cells to a certain degree[11-14].

As an indispensable signaling pathway in the body, the VEGF-Notch signaling pathway plays pivotal regulatory roles in the physiological and pathological processes of glaucoma, especially neovascular glaucoma, such as cell proliferation, apoptosis and angiogenesis[15-17]. Under the circumstance of acute intraocular hypertension, such core molecules as VEGF, Notch1 and Notch2 in the VEGF-Notch signaling pathway can be overexpressed. This may activate the VEGF-Notch signaling pathway. Subsequently, the pathway regulates the expression of diverse downstream effectors closely associated with physiological and pathological processes such as apoptosis and angiogenesis, thereby affecting intraocular pressure and the apoptosis of retinal ganglion cells. Therefore, the VEGF-Notch signaling pathway is considered as a hot topic in glaucoma-induced acute intraocular hypertension.

In this study, our results revealed that the protein and mRNA expressions of VEGF, Notch1 and Notch2 were remarkably high in retinal tissues of glaucoma rats. It can be seen that in the case of glaucoma-induced acute intraocular hypertension, the transcriptional and translational levels of VEGF, Notch1 and Notch2 are markedly up-regulated. Therefore, the VEGF-Notch signaling pathway is obviously activated. This may be a vital pathological mechanism and factor leading to the apoptosis of retinal ganglion cells and the failure of reduction in intraocular pressure of glaucoma rats.

MiR-126, a key member of the miRNA family in the body, is an important upstream regulatory factor that modulates cell proliferation, apoptosis and several downstream signaling pathways. Current studies[18-20] have demonstrated that miR-126 is highly expressed in retinal tissues of glaucoma rats. It is also closely correlated with the apoptosis of retinal ganglion cells. This is similar to the results of this study that miR-126 was abnormally expressed in retinal tissues of glaucoma rats. To continuously explore its related mechanism, miR-126 antagomir was used as a control in this work. After miR-126 antagomir was transfected to inhibit miR-126 expression, the abnormally high expressions of VEGF, Notch1 and Notch2 proteins and mRNAs were evidently down-regulated in retinal tissues of glaucoma rats. This indicates that the VEGF-Notch signaling pathway is suppressed. In the meantime, the apoptosis rate of retinal ganglion cells declined remarkably, implying that miR-126 antagomir suppresses the apoptosis of retinal ganglion cells and lowers intraocular pressure. All these results suggested that miR-126 antagomir exerted a protective effect in the antagomir-miR-126 model with regards to glaucoma-induced acute intraocular hypertension model.

Conclusions

The novelty of this study was that miR-126 facilitates the apoptosis of retinal ganglion cells in glaucoma rats by promoting the VEGF-Notch signaling pathway.

Conflict of Interests

The authors declare that they have no conflict of interest.

References

1) Qin VL, Kaleem M, Conti FF, Rockwood EJ, Singh A, Sood-Mendiratta S, Sears JE, Silva FQ, Eisengart J, Singh RP. Long-term Clinical Outcomes of Pars Plana Versus Anterior Chamber Placement of Glaucoma Implant Tubes. J Glaucoma 2018; 27: 440-444.
2) Krzyzanowska-Berkowska P, Melinska A, Helemejko I, Robert ID. Evaluating displacement of lamina cribrosa following glaucoma surgery. Graefes Arch Clin Exp Ophthalmol 2018; 256: 791-800.
3) Quigley HA. Glaucoma. Lancet 2011; 377: 1367-1377.
4) Suwan Y, Fard MA, Geyman LS, Tantraworasin A, Chui TY, Rosen RB, Ritch R. Association of myopia with peripapillary perfused capillary density in patients with glaucoma: an optical coherence tomography angiography study. JAMA Ophthalmol 2018; 136: 507-513.
5) Heijl A. Glaucoma treatment: by the highest level of evidence. Lancet 2015; 385: 1264-1266.
6) Zeng W, Lin Y, Lin H, Wu X. Silencing NEAT1 suppresses thyroid carcinoma via miR-126/NEAT1/VEGFA axis. Front Biosci (Landmark Ed) 2020; 25: 564-576.
7) Ando Y, Yamazaki M, Yamada H, Munetsuna E, Fujii R, Mizuno G, Ichino N, Osakabe K, Sugimoto K, Ishikawa H, Ohashi K, Teradaira R, Ohta Y, Hamajima N, Hashimoto S, Suzuki K. Association of circulating miR-20a, miR-27a, and miR-126 with non-alcoholic fatty liver disease in general population. Sci Rep 2019; 9: 18856.
8) Wu Z, Medeiros FA. Sample size requirements of glaucoma clinical trials when using combined optical coherence tomography and visual field endpoints. Sci Rep 2019; 9: 18886.

9) Occhiutto ML, Maranhao RC, Costa VP, Konstas AG. Nanotechnology for medical and surgical glaucoma therapy-a review. Adv Ther 2020; 37: 155-199.
10) Enoch J, Jones L, Taylor DJ, Bronze C, Kirwan JF, Jones PR, Crabb DP. How do different lighting conditions affect the vision and quality of life of people with glaucoma? A systematic review. Eye (Lond) 2020; 34: 138-154.
11) Torres LA, Sharpe GP, Hutchison DM, Zangalli CS, Burk RO, Reis A, Costa VP, Nicolela MT, Chauhan BC, Vianna JR. Influence of Bruch's membrane opening area in diagnosing glaucoma with neuroretinal parameters from optical coherence tomography. Am J Ophthalmol 2019; 208: 94-102.
12) Lenzhofer M, Strohmaier C, Sperl P, Hohensinn M, Hitzl W, Steiner V, Moussa S, Motloch K, Baca B, Krall E, Reitsamer HA. Effect of the outer stent position on efficacy after minimally invasive transscleral glaucoma gel stent implantation. Acta Ophthalmol 2019; 97: e1105-e1111.
13) Daneshvar R, Yarmohammadi A, Alizadeh R, Henry S, Law SK, Caprioli J, Nouri-Mahdavi K. Prediction of glaucoma progression with structural parameters: comparison of optical coherence tomography and clinical disc parameters. Am J Ophthalmol 2019; 208: 19-29.
14) Choudhari NS, Mundhe G, Khanna R, Rathi V, Garudadri CS. toward better health outcomes in rural and under-served areas: L. V. prasad eye institute's diagonal model of glaucoma care. Ophthalmic Epidemiol 2019; 26: 420-429.
15) Wang P, Zhu S, Yuan C, Wang L, Xu J, Liu Z. Shear stress promotes differentiation of stem cells from human exfoliated deciduous teeth into endothelial cells via the downstream pathway of VEGF-Notch signaling. Int J Mol Med 2018; 42: 1827-1836.
16) Li S, Xu G, Gao F, Bi J, Huo R. Erratum: expression and association of VEGF-Notch pathways in infantile hemangiomas. Exp Ther Med 2018; 16: 3752.
17) Deng S, Zeng Y, Wu L, Hu Z, Shen J, Shen Y, Shen Y, Zhou Y, Chen J, Lin S. The regulatory roles of VEGF-Notch signaling pathway on aplastic anemia with kidney deficiency and blood stasis. J Cell Biochem 2018: (DOI: 10.1002/jcb.27516).
18) Xiao J, Lai H, Wei SH, Ye ZS, Gong FS, Chen LC. LncRNA HOTAIR promotes gastric cancer proliferation and metastasis via targeting miR-126 to active CXCR4 and RhoA signaling pathway. Cancer Med 2019; 8: 6768-6779.
19) Rouigari M, Dehbashi M, Tabatabaeian H, Ghaedi K, Mohammadynejad P, Azadeh M. Evaluation of the expression level and hormone receptor association of miR-126 in breast cancer. Indian J Clin Biochem 2019; 34: 451-457.
20) Pedini F, De Luca G, Felicetti F, Puglisi R, Boe A, Arasi MB, Fratini F, Mattia G, Spada M, Caporali S, Biffoni M, Giuliani A, Care A, Felli N. Joint action of miR-126 and MAPK/PI3K inhibitors against metastatic melanoma. Mol Oncol 2019; 13: 1836-1854.